Interaction of GaSe with GaAs(111): Formation of heterostructures with large lattice mismatch

Lee E. Rumaner[a)]
Department of Materials Science and Engineering, University of Washington, Seattle, Washington 98195

Marjorie A. Olmstead
Department of Physics, University of Washington, Seattle, Washington 95195

Fumio S. Ohuchi[b)]
Department of Materials Science and Engineering, University of Washington, Seattle, Washington 98195

(Received 19 June 1997; accepted 27 February 1998)

We have studied the epitaxial growth of GaSe, a layered van der Waals material, on GaAs, a zinc-blende-structure semiconductor. This heterostructure exhibits a 6% lattice mismatch, and is a prototypical example of van der Waals epitaxy, where the weak van der Waals interaction allows the misfit to be accommodated without the formation of electronically active defects. GaSe was supplied to the growing surface from a single GaSe Knudsen cell. Reflection high energy electron diffraction and x-ray photoemission spectroscopy studies of the nucleation of GaSe indicate Se reacts with the GaAs surface to remove the surface dangling bonds prior to GaSe formation. This is followed by the oriented growth of stoichiometric GaSe layers, that are rotationally aligned with the underlying GaAs substrate. The termination of the GaAs dangling bonds most likely occurs by Se substitution for As in the surface layer of GaAs(111) *B* and by direct bonding of Se to surface Ga on GaAs(111) *A* surfaces. In addition, photoemission measurements indicate that the subsurface Se uptake into the GaAs(111) *A* lattice is higher than that in the (111) *B* lattice. © *1998 American Vacuum Society.* [S0734-211X(98)10503-6]

I. INTRODUCTION

The heteroepitaxy of thin films has resulted in the development of novel semiconductor devices and has led to observation of new physical phenomena. However, the need for lattice matching between the materials forming a heterostructure severely limits material selection. van der Waals epitaxy (VDWE) is a method used to overcome both lattice and thermal expansion mismatch limitations.[1–8] In VDWE, epitaxial layers are grown on surfaces for which the absence of dangling bonds leads to growth dominated by van der Waals forces. For example, layered materials such as metal chalcogenides exhibit VDWE. In this work, we address the growth of such a layered material, GaSe, on a covalently bonded semiconductor, GaAs.

The layer of GaSe consists of four two-dimensional (2D) monoatomic sheets in a sequence of Se–Ga–Ga–Se, where atoms within each layer are tightly bound with a mixture of covalent and ionic bonds, and the layers are held by van der Waals force.[9] GaSe has highly anisotropic transport, mechanical, and optical properties,[10] and especially important, possesses high nonlinear optical coefficients in the infrared ranges, making it a candidate for second harmonic generation (SHG) materials.[11–13] Interest for this use has led to a conceited effort to fabricate bulk single crystals of GaSe, and many of its optical and electrical properties have been investigated.[14]

The VDWE technique has recently been applied to the growth of a layered material on hexagonally symmetric, three-dimensional (3D) substrates such as GaAs(111)[15–22] and Si(111),[23–30] where the van der Waals interaction is believed to occur between the passivated substrate and the inert surface of the layered material. It has been suggested that termination of the surface dangling bonds is a necessary condition for initiating the growth of a van der Waals material on a surface exhibiting dangling bonds.[15] In the case of GaAs, this has been accomplished *ex situ* using S from a $(NH_4)_2S_x$ solution[15] and *in situ* using an overpressure of Se prior to growing the van der Waals layer, where it was postulated that the active bonds on the GaAs surface were removed by reaction of the substrate with Se prior to the formation of GaSe.[12,17] However, no detailed study confirming this termination process has been reported.

In previous studies of GaSe growth on untreated GaAs substrates were used separate Ga and Se sources with an overpressure of Se to facilitate Se termination of the GaAs surface.[16–19] Thus, while these studies suggest that Se termination is sufficient to enable uniform GaSe growth on GaAs, they do not address its necessity. In this study, single domain GaSe layers have been grown on GaAs(111) *A* and *B* from a single GaSe Knudsen cell. In addition to the difference in stoichiometry, the single source also results in different incident species. In the case of separate sources, Ga and Se_x are the dominant species, where x depends on whether or not the Se is excited by a heated filament or cracker. For a single GaSe source, however, the incident species are a mixture of Ga_2Se and Se_2.[31] It is thus possible for free Se from Se_2 to terminate the GaAs surface prior to growth while the Ga_2Se either does not stick or accumulates as Ga-rich material.

a)Present address: Intel Corporation, Santa Clara, CA 95052.
b)Electronic mail: ohuchi@u.washington.edu

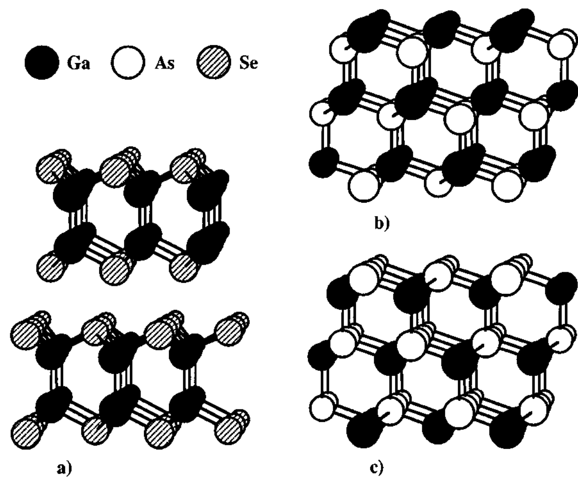

FIG. 1. Ideal structure of (a) GaSe(0001), (b) GaAs(111) *A*, and (c) GaAs(111) *B* surfaces, viewed 4° from the [$\bar{1}$10].

However, it is also possible that Ga_2Se and Se_2 will recombine at the substrate surface and form GaSe or Ga_2Se_3 without reacting with the substrate surface. If Se termination of the GaAs surface were not necessary for GaSe growth, use of a single GaSe source without a Se overpressure should form stoichiometric GaSe from the first layer. On the other hand, if the chemical forces driving the exchange of As with Se dominate over the formation of GaSe at the GaAs surface, then the initial deposition will be Se rich. In this article, we report *in situ* reflection high energy electron diffraction (RHEED) and x-ray photoemission spectroscopy (XPS) studies of this deposition process.

Ideally terminated GaAs(111) *A* and *B* surfaces are shown in Fig. 1, along with GaSe(0001). The GaAs(111) *A* surface is Ga terminated, with the 2×2 surface reconstruction believed to consist of an ordered array of Ga vacancies.[32–34] The removal of one quarter of the Ga atoms leaves the unit cell with an even number of electrons and no partially filled orbitals. On this surface we find an extensive uptake of Se, both forming an additional layer at the surface and replacing the substrate As prior to the deposition of stoichiometric GaSe. The GaAs(111) *B* surface is As terminated, with the reconstruction depending on the local As concentration.[35,36] Under our preparation conditions (that will be described in Sec. II) the local stoichiometry and reconstruction are likely close to that of the $\sqrt{19}\times\sqrt{19}$ structure.[37] On this surface we observe an uptake of approximately one monolayer (ML) of Se prior to the deposition of GaSe. For both substrate orientations, we observe a smoothing of the surface by this initial reaction. We also observe complete coverage of the GaAs substrate by a film with the GaSe lattice constant after deposition of the first one or two GaSe layers.

II. EXPERIMENTAL PROCEDURE

GaSe (99.99% purity) was sublimed from a single Knudsen cell. A temperature programmed desorption mass spectrometry study has shown that GaSe sublimates as a combination of Ga_2Se and Se_2.[31] The deposition rate was measured with a previously calibrated deposition thickness monitor and the molecular beam was maintained at a constant flux. In the following, equivalent thicknesses are quoted assuming this constant growth rate of 1.0 ML/min, where 1 ML is a GaSe molecular layer, containing two atomic layers each of Ga and Se (see Fig. 1). The layer spacing in bulk GaSe is 0.8 nm for a growth rate of 0.13 Å/s. The growth rate was calibrated using a GaAs(111) *B* substrate. The deposition chamber base pressure was maintained at 2×10^{-9} Torr. A Thermionics/Veetech (VE-052) RHEED system operated at 20 kV was used to monitor the deposition process *in situ*. The diffraction pattern was observed on a standard phosphor screen and recorded with a charge coupled device (CCD) camera.

Two different surface conditions were used in this study: GaAs(111) *A* (a Ga-rich surface) and GaAs(111) *B* [an As-rich surface, also referred to as GaAs($\bar{1}\bar{1}\bar{1}$)]. In all cases, an *n*-type GaAs wafer (1 cm×2 cm) was mounted on a thin Mo sheet using Ga. The Mo sheet was then attached to a stainless steel sample holder cassette that could be transferred under ultrahigh vacuum (UHV) from the deposition chamber to the analytical chamber. The samples were heated from the back by radiation from a Ta heater wire. The sample temperature was measured using a thermocouple attached to the front side of the sample holder cassette, adjacent to the sample. The desorption temperature of the GaAs surface oxide at 600 °C was used to calibrate this thermocouple, as well as a thermocouple mounted directly on the front of a special GaAs sample.

Using a single GaSe source and maintaining a constant flux, the substrate temperature becomes the critical parameter for growing oriented, single domain GaSe. If the temperature is too high, the GaSe desorbs from the surface and no layer is formed. If the temperature is too low, then multigrained or amorphous layers are formed. In this research, it was found that single orientation, stoichiometric GaSe (as indicated by RHEED and XPS) could be formed within a temperature range from 480 to 540 °C. In the results reported below, GaSe was deposited on the surfaces of GaAs(111) *A* and *B* at approximately 530 °C. Transmission electron microscopy and atomic force microscopy measurements under similar growth conditions confirm the growth of layered GaSe.[22]

After each stage of deposition, the samples were cooled to room temperature and transferred in vacuum to an analytical chamber for XPS. XPS was performed using Al K_α x rays (1486 eV) and detected using a double pass cylindrical mirror analyzer (CMA). Detailed XPS scans of the Ga, As, and Se 3*d* regions were acquired at a pass energy of 25 eV. Binding energies are reported relative to the Fermi level, calibrated with Au $4f_{7/2}$ emission at 84.0 eV. Following the measurement, the sample was transferred in vacuum back to the VDWE chamber for further growth. The samples showed negligible accumulation of carbon or oxygen during this procedure, as was indicated by the XPS results.

Photoemission spectra of the As, Se, and Ga 3*d* core levels are complicated by the presence of satellite structures.

The photoemission plasmon satellites of the Ga and As 3d peaks lie close in energy to the As and Se 3d peaks, respectively (see Figs. 4 and 8), and Se and As 3d emissions excited by satellites in the unmonochromatized Al $K\alpha$ x rays partially overlap the main As and Ga 3d peaks. The contributions by the x-ray satellites were removed by a Fourier transform method before further analysis (they are removed in Figs. 4, 5, 8, and 9). The spectra were fitted with line shapes derived from the bulk GaAs and GaSe data. This both inherently included any photoemission satellites and accounted for the expected stoichiometry of the substrate and overlayer. We also fitted the data using Voigt doublets for the main components and a broad Gaussian for the plasmon satellites, and found consistent results.

III. RESULTS

In the following, we present the data from RHEED and XPS experiments during the growth of GaSe thin films on thermally cleaned As- and Ga-terminated GaAs(111) surfaces.

A. GaSe growth on an As-terminated GaAs(111) *B* surface

Figures 2(a)–2(e) show the RHEED patterns taken from the thermally cleaned GaAs(111) *B* surface before deposition and after a half, one, two, and four layers of GaSe deposition. The sample orientation is identical in all cases, with the RHEED beam directed along GaAs[$\bar{1}$10].

To remove the surface oxide, the substrate was initially heated to approximately 600 °C without an As overpressure. This results in the loss of As from the surface and atomic scale roughening.[38] This roughened surface is apparent in the RHEED pattern shown in Fig. 2(a), where transmission diffraction through the asperities results in a spot pattern. Locally, however, the surface may be similar to the $\sqrt{19}\times\sqrt{19}$ structure, which consists of approximately 2/3 Ga and 1/3 As in hexagonal rings above a completely As-terminated layer.[35] Upon exposure to less than 1 ML of GaSe [Fig. 1(b)], the surface appears smoother: the RHEED pattern is more distinct and streaks start to form over the spotly pattern. Streaks are known to result from flattening of asperities on the surface and are an indication of surface disorder.[39] The spacing between streaks is inversely proportional to the surface lattice constant, which is 6% larger in GaAs than in GaSe.

While it is difficult to observe a difference between the streak and spot spacings in the pattern itself, a shift is apparent in the average of the digitized RHEED intensity along the [111] axis (streak direction). Figure 3 shows such RHEED profile plots for each image in Fig. 2, with the expected peak positions for GaAs and GaSe RHEED patterns indicated. The formation of a new peak near the expected GaSe position is apparent after a half layer of growth. This indicates that the deposited GaSe attains its own lattice constant in the first layer, rather than straining to match the GaAs substrate. As is evident from the patterns, the GaSe layer is oriented with the major symmetry axis parallel to the GaAs surface. In addition, only a single GaSe orientation is observed.

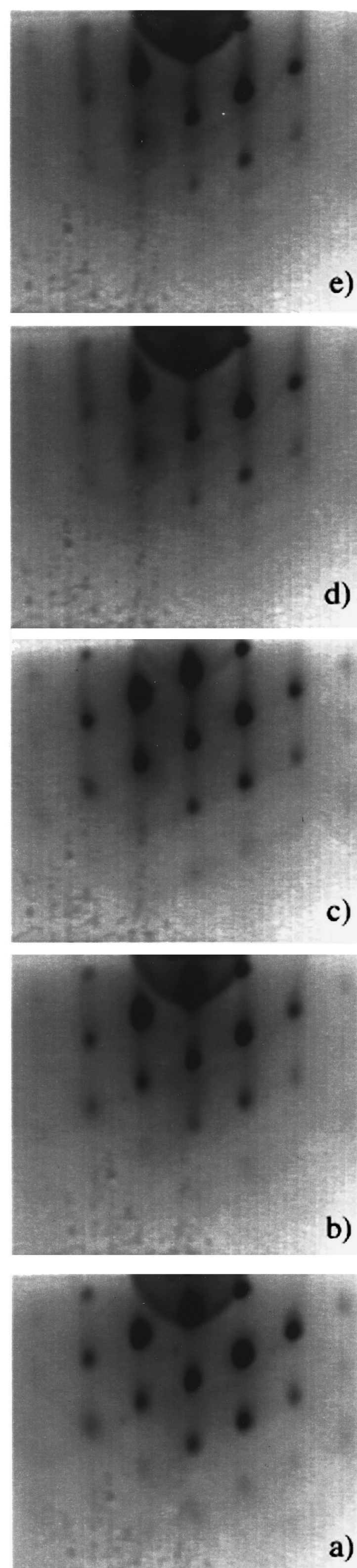

FIG. 2. RHEED patterns taken from a GaAs(111) *B* substrate (a) before deposition and after (b) 1/2, (c) one, (d) two, and (e) four layers of GaSe deposition. The RHEED beam is in the GaAs[$\bar{1}$10] orientation.

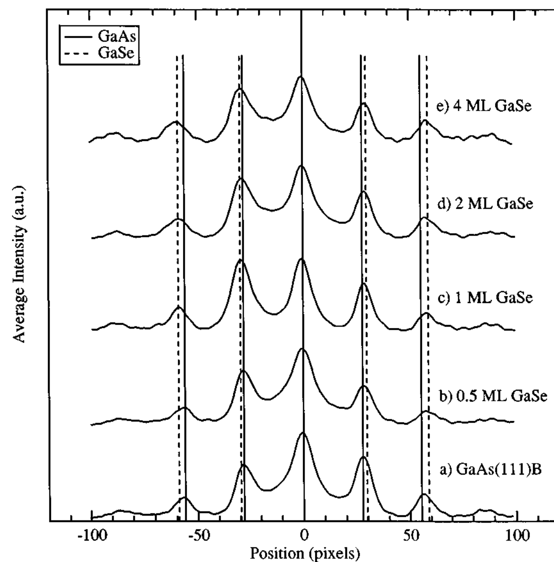

FIG. 3. RHEED intensity profile plot of the images in Fig. 2. The solid lines indicate the expected peak positions for GaAs while the dotted line indicates that expected for GaSe. These plots were obtained by averaging the intensity in the vertical (111) direction after background subtraction. The asymmetry in the RHEED pattern is due to degradation of the phosphor screen and is not related to the deposition.

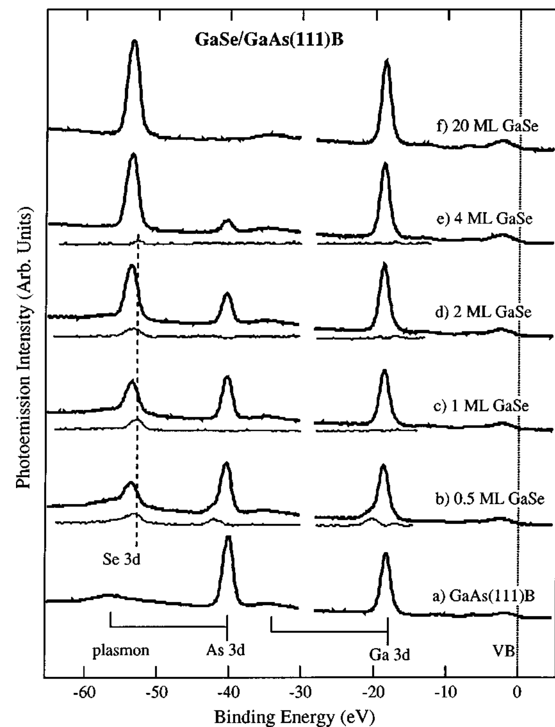

FIG. 4. Photoemission spectra of the shallow core (Ga, As, and Se $3d$) and valence band regions for the GaAs(111) B substrate (a) before deposition and after (b) 1/2, (c) one, (d) two, (e) four, and (f) 20 layers of GaSe deposition. The interface contribution is plotted below curves (b)–(e) (see the text). The dotted line highlights the emission from excess Se at the interface.

Further exposure to GaSe changes the RHEED pattern [Figs. 2(c)–2(e)]. After one layer of GaSe deposition, diffraction patterns generated from both GaSe and GaAs are apparent, with the GaSe signal more intense than the GaAs signal. The RHEED profile scans show mainly GaSe diffraction above 1 ML. The full patterns show that the transmission diffraction spots disappear slowly, with some contribution even after four layers (3.2 nm) of deposition. Since each GaSe layer is four atoms thick (0.8 nm), observation of any signal due to GaAs above 1–2 ML coverage is indicative of either regions of uncovered GaAs or transmission through GaAs asperities. Eventually, however, the GaSe fills in the roughness of the GaAs substrate.

Figure 4 shows photoemission spectra from the shallow core levels and valence bands for the same depositions of GaSe on GaAs(111) B as in Figs. 2 and 3. Also plotted in Fig. 4 is the estimated interface contribution to the spectra, obtained as follows. Data in the energy range -47 to -14 eV (Ga and As peaks) were fitted to a sum of bulk GaAs [curve (a)] and GaSe [curve (f)] line shapes. The sum of the bulk GaAs and GaSe components was then subtracted from the entire spectrum, and the difference between the data and the fit is plotted beneath each spectrum in Fig. 4. The energy positions of the various components are listed in Table I and the intensities are shown later in Fig. 10. An overall shift of 0.4 eV to higher binding energy was observed in the bulk GaAs peaks following the deposition of GaSe. For films at least 1 ML thick, excess Se was observed, but there was no indication of additional Ga or As components. For 0.5 ML deposition, however, additional components were present for all three species.

Ga, As, and Se $3d$ spectra for 0.5 ML GaSe/GaAs(111) B are shown enlarged in Fig. 5. Due to the small energy differences among some of the components, the spectra were fitted self-consistently as follows: The Ga and As peaks were fit simultaneously to two GaAs line shapes and one GaSe line shape. The GaSe line shape was then fixed in position and amplitude while a 10 eV wide region centered on the As peak was fitted with two GaAs line shapes. The As was fitted first since the only source of As is the original crystal. Next, the Ga peak was fitted to two GaAs line shapes and one GaSe line shape, with the bulk GaAs contribution fixed at the position and amplitude obtained fitting the As $3d$. Finally, the Se $3d$ was fitted: Two GaAs line shapes were fixed at the values obtained fitting the As $3d$ (to yield the proper As plasmon intensity) and the bulk GaSe line shape was fixed at the value obtained fitting the Ga $3d$; two additional GaSe line shapes were also required to fit the Se $3d$ region. The spectra are aligned in Fig. 5 so that GaAs components of the As $3d$ and Ga $3d$ are at the same energy, as are the GaSe components of the Se $3d$ and Ga $3d$ peaks. The splitting between the GaAs and GaSe peaks (Ga $3d$) is 0.2 ± 0.1 eV (see Table I). By comparing the GaAs [Fig. 4(a)] and the GaSe [Fig. 4(f)] spectra, we find that the splitting between the Ga $3d$ and the valence band maximum is 0.15 eV larger for GaSe than it is for GaAs. The observed energy difference in the Ga $3d$ thus implies that the valence band offset is close to zero.

For 0.5 ML of GaSe on GaAs(111) B, the Se, As, and Ga $3d$ peaks all contain small contributions at a binding en-

TABLE I. Binding energy peak positions (eV) for GaSe growth on GaAs(11) *A* and GaAs(111) *B* measured relative to the Fermi level (bulk components) or to the relevant bulk peak (interface components). Values are ± 0.1 eV.

GaAs(111) *B*	GaAs	1/2 layer	1 layer	2 layers	4 layers	20 layers
GaAs (Ga peak)	−19.1	−19.5	−19.4	−19.4	−19.5	
GaSe (Ga peak)		−19.7	−19.6	−19.6	−19.6	−19.4
Excess Se		+0.5	+0.6	+0.2	+0.8	
(relative to GaSe)		−1.6				
Excess As		−1.8				
(relative to GaAs)						
Excess Ga		−1.8				
(relative to GaAs)						
GaAs(111) *A*	GaAs	1/2 layer	1 layer	2 layers	4 layers	15 layers
GaAs (Ga 3*d*)	−19.2	−19.2	−19.5	−19.5	−19.5	
GaSe (Ga 3*d*)		−19.8	−20.1	−19.8	−19.7	−19.6
Excess Se		+0.8	+0.9	+0.8	+0.6	
(relative to GaSe)						

ergy of -1.8 eV relative to the bulk GaAs position. These contributions are not present in any other spectra, and we associate them with the region of the GaAs surface that has partially reacted with the incident Ga_2Se and Se_2, but on which bulk GaSe has not yet nucleated. If they persisted underneath GaSe, they would still be observable at 1 ML deposition. By using line shapes for bulk GaAs and GaSe, the fitted intensities of the As and Se peaks are found relative to the amount of Ga in a stoichiometric compound. In these units, the relative intensity of these high binding energy components is 1.0:0.7:0.5 for Ga:As:Se.

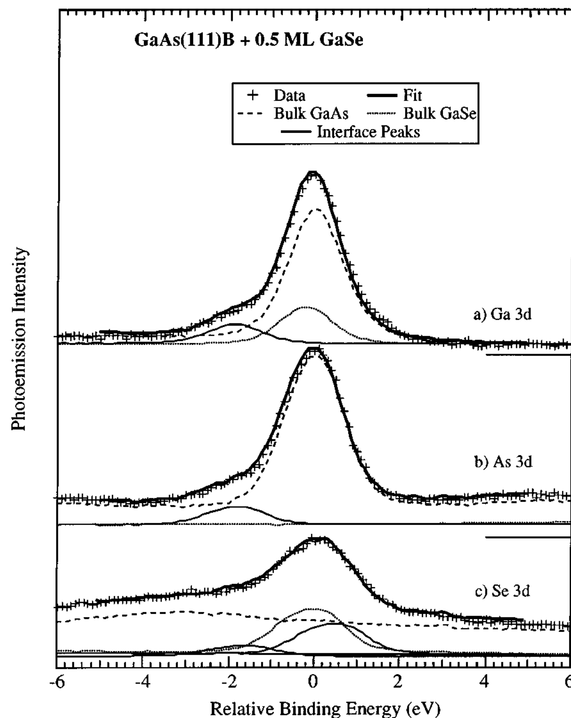

FIG. 5. Photoemission spectra for the (a) Ga 3*d*, (b) As 3*d*, and (c) Se 3*d* regions for 0.5 molecular layers of GaSe on GaAs(111) *B*. The data (+) are fitted with the sums of the bulk line shapes (see the text), and are plotted with the same intensity scale. The peaks are plotted relative to the bulk GaAs peak position. The CMA axis was 45° from the sample normal.

The Se 3*d* exhibits a second component associated with the interface between GaSe and GaAs. This component has a binding energy about 0.5 eV lower than that of the GaSe overlayer, and it persists as the GaSe film grows thicker (see Fig. 4). The intensity of this peak is about 70% of the bulk GaSe component at 0.5 ML. After deposition of an additional 0.5 ML of GaSe, the absolute intensity of the low-binding-energy peak increased, but the relative intensity decreased to about 50% of the GaSe intensity. Each molecular layer of GaSe consists of two Ga and two Se atomic layers (see Fig. 1), so a single Se atomic layer buried at the interface should contribute less than 50% of the GaSe intensity due to attenuation by inelastic scattering.

Continued deposition beyond 1 ML leads to decay of the substrate GaAs and interface Se emission, whereas the GaSe contribution grows. The energy difference between the GaAs and GaSe components in the Ga 3*d* decreases to about 0.0 eV, indicating that the GaSe valence band maximum (VBM) is slightly above the GaAs VBM and the band alignment is staggered, although the results are within the error bars of a degenerate VBM.

B. GaSe growth on a Ga-terminated GaAs(111) *A* surface

An identical experiment was conducted using a GaAs(111) *A* (Ga-terminated) substrate. The starting surface was again prepared by annealing a commercial wafer in UHV, but this process leads to less roughening on the (111) *A* surface than on the (111) *B* surface. The native reconstruction of GaAs(111) *A* consists of one Ga vacancy per 2×2 unit cell, which leads to a nonpolar surface without dangling bonds.[32,33] Se interactions with this surface are expected to be quite different from those with the (111) *B* surface, since there is no surface As to undergo an exchange reaction and the empty Ga 3*s* orbitals may serve as bonding sites for the

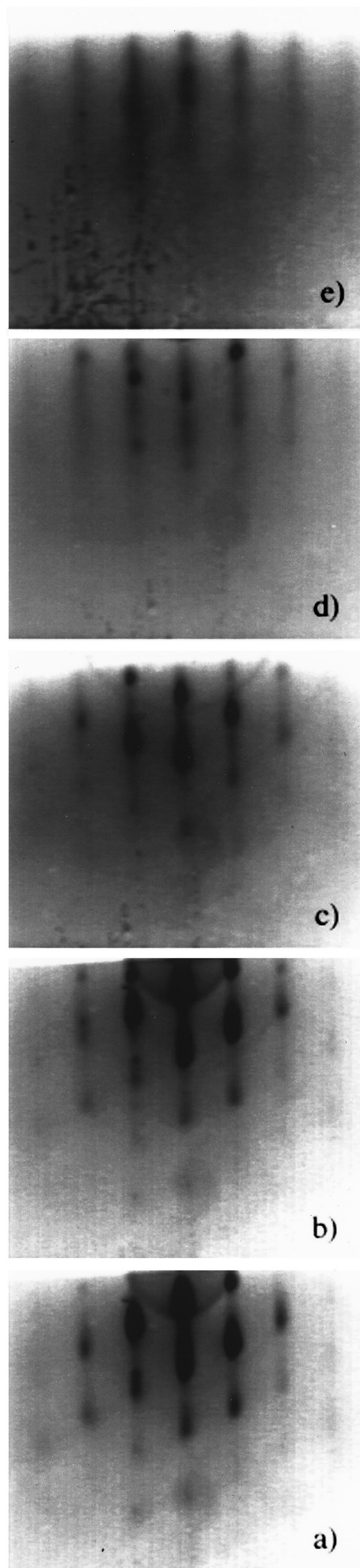

FIG. 6. RHEED patterns taken from a GaAs(111) A substrate (a) before deposition and after (b) 1/2, (c) one, (d) two, and (e) four layers of GaSe deposition. The RHEED beam is in the GaAs[$\bar{1}$10] orientation.

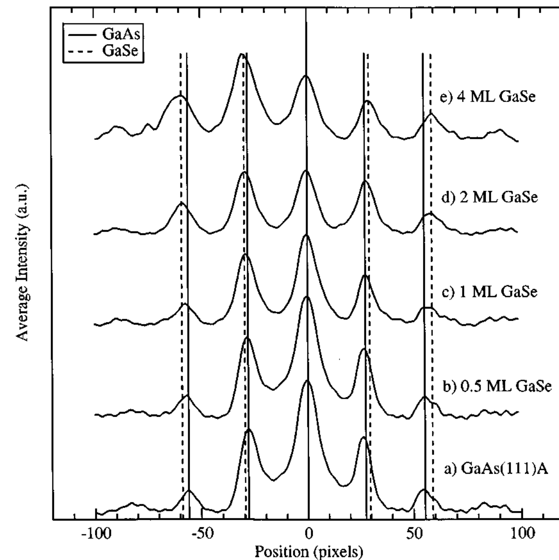

FIG. 7. RHEED intensity profile plot of the images in Fig. 6. The solid lines indicate the expected peak positions for GaAs while the dotted line indicates that expected for GaSe. These plots were obtained by averaging the intensity in the vertical (111) direction after background subtraction. The asymmetry in the RHEED pattern is due to degradation of the phosphor screen and is not related to the deposition.

Se 3s lone-pair electrons. In addition, the open structure created by the Ga vacancies may enhance Se interdiffusion into the GaAs substrate.

The RHEED data for a sequence of depositions on GaAs(111) A are shown in Fig. 6. Similar to GaAs(111) B, the substrate RHEED pattern is gradually replaced by streaks associated with the oriented GaSe film. A noticeable difference from the (111) B surface is the initial substrate pattern itself [Fig. 6(a)], which is composed of elongated spots characteristic of a small amount of surface roughness. This is in contrast to the sharp transmission diffraction spots observed for the (111) B substrate. No microstructural comparison of the difference in substrate surface roughness has been made; however, it is assumed that the surface Ga layer decreases the loss of As and minimizes the effect of thermal roughening.

After deposition of a half layer of GaSe on GaAs(111) A, a new diffraction pattern associated with GaSe is observed [Fig. 6(b)]. Further growth results in the clear formation of GaSe, rotationally aligned with the GaAs substrate. The existence of a distinct overlayer lattice constant near the expected value for GaSe is visible in the vertically integrated RHEED intensity profile shown in Fig. 7. The principal difference from the (111) B case is a more rapid decay of the substrate pattern with overlayer thickness, indicating a more uniform (or thicker) overlayer coverage.

Figure 8 shows photoemission spectra from the shallow core levels and valence bands for the same depositions of GaSe on GaAs(111) A as for Figs. 6 and 7. The estimated interface contribution, found by subtracting the bulk GaAs and GaSe contributions from the data in a similar manner to Fig. 4, is also plotted. Unlike the case for (111) B, the only component other than those associated with the stoichio-

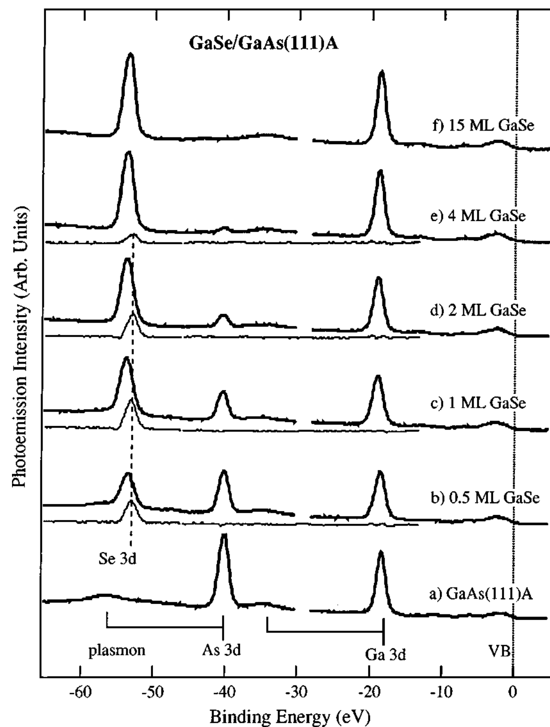

FIG. 8. Photoemission spectra of the shallow core (Ga, As, and Se $3d$) and valence band regions for the GaAs(111) A substrate (a) before deposition and after (b) 1/2, (c) one, (d) two, (e) four, and (f) 20 layers of GaSe deposition. The interface contribution is plotted below curves (b)–(e) (see the text). The dotted line highlights the emission from excess Se at the interface.

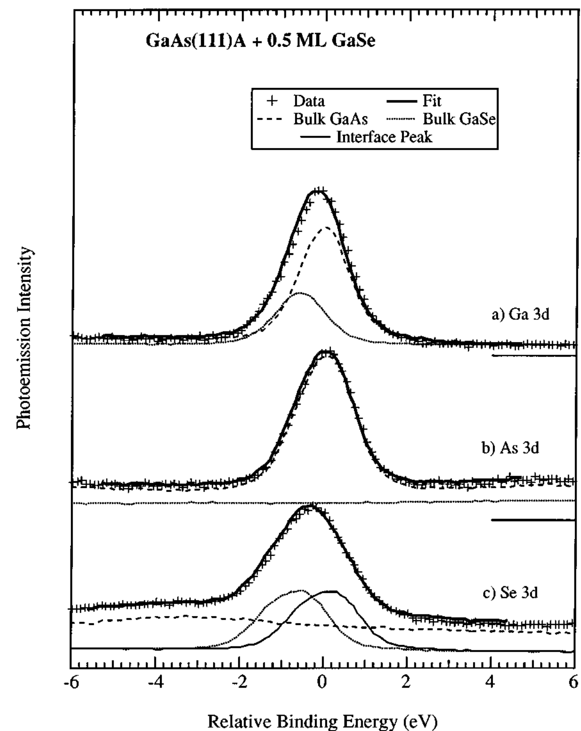

FIG. 9. Photoemission spectra for the (a) Ga $3d$, (b) As $3d$, and (c) Se $3d$ regions for 0.5 molecular layers of GaSe on GaAs(111) B. The data (+) are fitted with the sums of the bulk line shapes (see the text), and are plotted with the same intensity scale. The peaks are plotted relative to the bulk GaAs peak position.

metric substrate or overlayer is a Se $3d$ component shifted to lower binding energy from the main GaSe peak for films $\leqslant 4$ ML. Table I lists the positions of the fitted peaks, and the intensities are plotted later in Fig. 10. For the same GaSe exposure (flux×time), the (111) A substrate shows less As and more Se emission (both as GaSe and as excess Se) than the (111) B substrate, indicating a thicker film and a higher initial sticking coefficient.

An expanded plot of the spectra for a nominal deposition of 0.5 ML GaSe on GaAs(111) A is shown in Fig. 9. In contrast to the (111) B substrate, there is no clear component at higher binding energy (HBE) from the main components on any of the peaks. The As $3d$ is consistent with a single bulk GaAs component, whereas the Ga $3d$ is composed of GaAs and GaSe components. The separation between the Ga components is larger here than in the (111) B case: 0.7 as opposed to 0.2 eV, implying a larger initial valence band offset of about 0.5 eV. A small HBE component might be present in the Ga $3d$ emission, as indicated by the slight deviation between the data and the fit on the high binding energy tail; the deviation could also be due to differences in inelastic scattering between the thick and thin films. It may also indicate a small amount of Ga_2Se present on the surface.

The Se $3d$ emission for 0.5 ML GaSe/GaAs(111) A can be decomposed into two nearly equal components, one at an energy consistent with GaSe and the other ~0.8 eV to lower binding energy. Similar to the (111) B case, this excess-Se component persists upon further deposition. Upon addition of 0.5 ML GaSe, its absolute intensity increases, although not as much as that of the GaSe-associated component (see Fig. 10). The excess-Se intensity then decreases as it is buried by the GaSe overlayer, as does the emission from the GaAs substrate. The energy difference between the GaAs and GaSe components decreases with increasing thickness toward a value of ~0.2 eV (and zero valence band offset).

IV. DISCUSSION

GaAs(111) A and (111) B substrates differ only in their surface structure and stoichiometry. Their symmetries and lattice spacings are identical, as are the underlying bulk properties such as the thermal expansion coefficient and the heat of formation. On both substrates, RHEED indicated the formation of oriented molecular layers with the GaSe lattice constant from the very first stages of deposition, and XPS showed the growth of stoichiometric GaSe once the initial layer was completed. This is strong evidence for van der Waals epitaxy of layered GaSe on GaAs(111) substrates for both surface orientations and demonstrates the possibility of merging layered materials with more traditional semiconducting and electronic materials.

The relative intensities of several photoemission components are shown in Fig. 10 as a function of thickness. The substrate GaAs contribution (from fitting the As peak) is seen to decay while the Se-related components increase. The total Ga signal shows a dip, followed by recovery as the

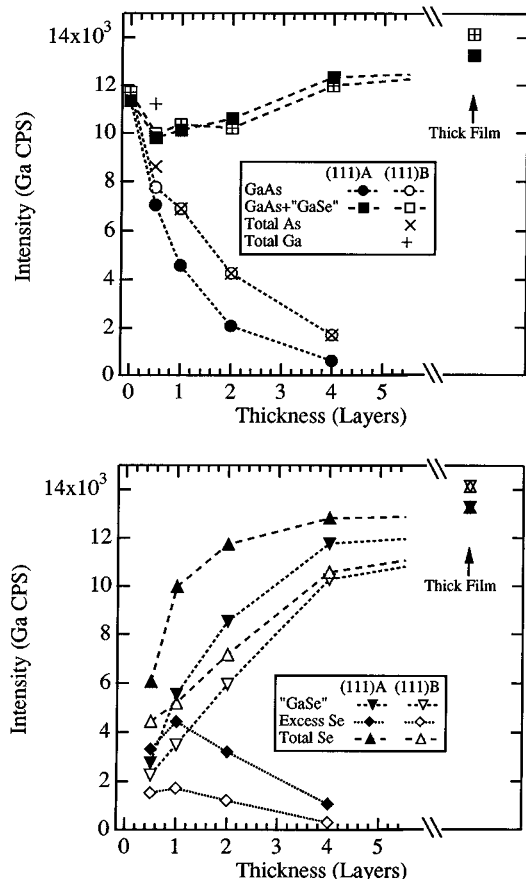

FIG. 10. Photoemission component intensity as a function of nominal film thickness for GaSe on GaAs(111) *A* (closed symbols) and on GaAs(111) *B* (open symbols). GaSe intensity refers to the Ga 3*d* intensity that is not directly associated with As, and may include some substrate Ga adjacent to interdiffused Se.

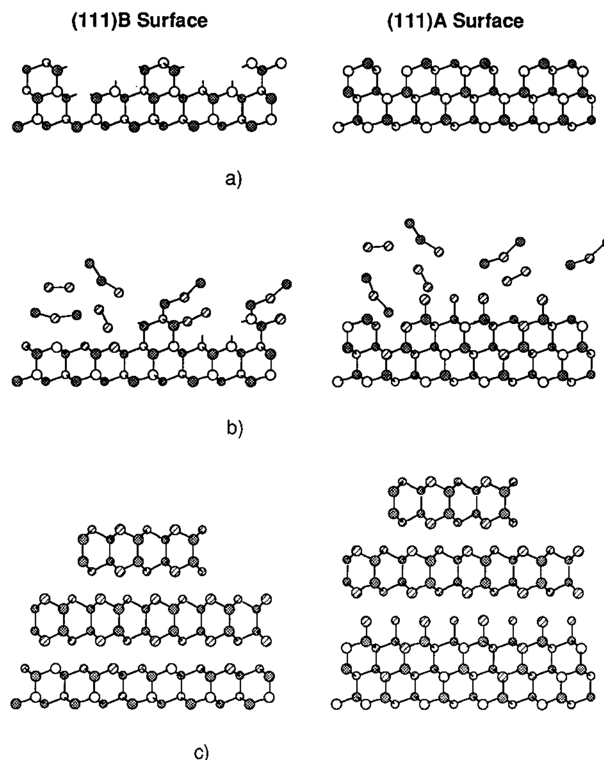

FIG. 11. Schematic diagram of the deposition and growth of GaSe on GaAs(111) *A* (right side) and on GaAs(111) *B* (left side). (a) Schematic of the initial substrate surface, (b) reaction of the surface to Ga_2Se and Se_2 incident beams, and (c) two layers of GaSe on the Se terminated GaAs(111) surface. Note the different locations of the Se termination for the two orientations and the enhanced Se interdiffusion into the GaAs(111) *A* surface.

substrate contribution is buried. We attempted to fit the data assuming laminar growth and a single escape depth, taking into account the variable take-off angles measured by the CMA (the CMA axis was 45° to the sample normal). It was not possible, however, to fit both the GaSe and total As intensities in this manner. This is consistent with the RHEED data, which indicate a rough surface.

While van der Waals epitaxy was achieved for both substrates, we observed significant differences in the growth of the first GaSe molecular layer on the GaAs(111) *A* and (111) *B* substrates. This indicates the importance of surface structure and stoichiometry in initiating GaSe growth on GaAs. The observed differences include (1) a higher sticking coefficient for Se-containing species on the (111) *A* surface than on the (111) *B*, (2) high binding energy photoemission components associated with the uncovered, reacted substrate on the (111) *B* surface that are absent from the (111) *A* surface at a comparable exposure to the incident flux, (3) a more rapid depletion of As emission on the (111) *A* surface than on the (111) *B* surface, and (4) a more rapid disappearance of the substrate RHEED patterns on the (111) *A* surface than on that of the (111) *B*.

The first observation, increased Se uptake by the (111) *A* surface relative to (111) *B* surface, has previously been observed for exposure of GaAs(111) to pure Se.[40] The simplest explanation of the more rapid disappearance of the substrate photoemission and RHEED signals on the (111) *A* surfaces is rapid burial of the substrate by a Se overlayer; we believe, however, that a combination of Se–As exchange and a different initial roughness of the substrate also play an important role. We attribute the HBE photoemission components to reactions of the incident Ga_2Se with the GaAs(111) *B* substrate.

A. Starting surface

Schematic diagrams of the GaAs(111) *A* and *B* surfaces and the subsequent growth of GaSe are shown in Fig. 11. The GaAs in this current study was thermally annealed without As or Se overpressure, resulting in thermal roughening and As evaporation. This results in a disordered surface layer with As surface vacancies and other defects, as is confirmed by the lack of a superstructure in the RHEED pattern. For the (111) *B* surface, the $\sqrt{19}\times\sqrt{19}$ reconstruction is predicted to be locally stable under Ga-rich conditions,[35] but the annealing has likely destroyed long-range order in the $Ga_{12}As_6$ rings on the surface and has created As vacancies in the first complete layer. This local roughness is shown schematically in Fig. 11(a) (left side).

In one model of van der Waals epitaxy on nonlayered

materials, chemical reactions are predicted to occur that will terminate the surface with fully occupied lone-pair orbitals, similar to those of the van der Waals layers. It is instructive to consider the surface stoichiometry required for such a surface. For the ideal (111) *B* surface, the top half of the double layer is occupied by As. To first order, the second layer Ga atoms each contribute an average of 3/4 electron per bond to each of three top layer atoms and the surface As has a partially occupied dangling bond orbital. The stable configuration for either As or Se in the top layer would be three back bonds (contributing an average of 5/4 electron each) to the second layer Ga plus a fully occupied lone-pair orbital, for a total of $5\,\frac{3}{4}$ electrons per surface atom. This average is obtained for a $GaSe_{0.75}As_{0.25}$ surface stoichiometry. In this configuration the Fermi level should be unpinned, since there would be no partially occupied orbitals near the surface.

For the (111) *A* surface, Ga occupies the top half of the double layer. Under Ga-rich conditions, the surface reconstructs with one Ga vacancy per 2×2 unit cell, shown schematically in Fig. 11(a) (right side). Electron counting arguments for this surface show the remaining three Ga atoms per unit cell as having empty surface orbitals and no dangling bonds, something that is likely to be true locally even in the absence of long-range order. There is thus no obvious reason for Se to bond to or replace As on this surface before growth of stoichiometric GaSe. Calculations for a 1×1 structure of monolayer S on GaAs(111) *A* support a site directly above the Ga atoms,[41] which results in a surface that is quite similar electronically to the GaAs(111) *B* surface.

B. Initial reaction

After the nominal deposition of 0.5 ML GaSe on GaAs(111) *B*, the photoemission spectra for all three elements (Ga, As, and Se) showed components of about 1.8 eV to higher binding energy than the bulk semiconductor. After the deposition of an additional 0.5 ML GaSe these components were not present. If the emitting species were trapped at the interface, they would have simply decreased in intensity with increased deposition; their disappearance indicates they are only present on the partially covered (111) *B* substrate. Such high-binding energy components were not observed after comparable deposition on the (111) *A* substrate, nor have they been observed for exposure of GaAs(111) [40] or GaAs(100)[40,42–44] to pure Se. We thus associate them with Ga_2Se interacting with the GaAs(111) *B* surface.

Under Ga-rich conditions, the clean (111) *B* surface forms $Ga_{12}As_6$ hexagonal rings above a completely As-terminated layer.[35] Even in the absence of an ordered reconstruction, these rings and other related structures likely provide reaction sites for Ga_2Se; in addition, sites due to the large thermal roughness on this surface also may be quite reactive. The measured intensity ratio of 1.0:0.7:0.5 for the Ga:As:Se in the high-binding energy peaks is consistent with Ga_2Se bonding to surface As, perhaps as an intermediate state before a Se–As replacement reaction is activated to form the nonreactive surface discussed above. The reaction may remove the surface asperities through etching with further exposure to GaSe. The large (1.8 eV) shift to higher binding energy may be attributed to a combination of the reduced screening in a moiety dangling from the substrate and a local shift in the Fermi energy. It is unlikely that oxygen or excess Se would lead to the same shift in all three core levels.

For deposition of GaSe on both GaAs(111) *A* and (111) *B*, there is excess Se over that expected for stoichiometric GaSe deposited on stoichiometric GaAs, with the effect much more pronounced on the (111) *A* surface. We begin with a stoichiometric GaSe single source that evaporates as $Ga_2Se_2 \Rightarrow Ga_2Se + \frac{1}{2}Se_2$,[31] and are able to grow stoichiometric GaSe once we are in a GaSe homoepitaxial regime. The observation of excess Se at low coverages thus indicates a higher sticking coefficient for Se_2 than for Ga_2Se during the initial interface formation. This Se may either replace near-surface As atoms or simply cover the GaAs substrate. On both surfaces, the Ga intensity decreases during deposition of the initial GaSe monolayer (see Fig. 10); if we exclude the peak associated above with Ga_2Se, the decrease and subsequent recovery are roughly the same on each surface. If Se simply replaced As or was deposited as stoichiometric GaSe, the number of Ga emitters within an inelastic decay length of the surface would not decrease;[45] Se must therefore be covering the GaAs substrate. The electron counting arguments and sulfur adsorption calculations described above predict 3/4 atomic layers of Se on the (111) *B* surface and a full layer on the (111) *A* one. The observed Ga decrease is consistent with these predictions.

Further evidence of Se termination is found in the change in band bending during growth of GaSe. Surface dangling bonds behave as electronic defects and act to pin the Fermi level near midband gap in GaAs.[40,46] As is seen in Fig. 12, this pinning results in band bending at the surface of the thermally cleaned GaAs(111) *B* substrate. In XPS, the binding energy is calculated as the energy difference between a given core level and the Fermi level (Fig. 12). For *n*-type GaAs, the pinning of the Fermi level at a location near the midband gap results in a decrease in the measured GaAs binding energy relative to an unpinned surface [Fig. 12(a)]. The shift of 0.4 eV in the GaAs binding energy after 0.5 ML GaSe deposition is evidence of the removal of midgap pinning states [Fig. 12(b)]. For the (111) *A* surface, the reduction in surface band bending does not occur until completion of the first GaSe layer. This is consistent with the S/GaAs(111) *A* calculations indicating the persistence of midgap states upon the addition of a group VI monolayer[41] and a gradual increase in the *n*-type doping of the near-surface region through Se–As exchange. The difference in valence band offset in the two cases also implies a different interface dipole.

The total Se uptake is much larger for the (111) *A* surface than for the (111) *B*. After 0.5 ML deposition of Ga_2Se_2 on the (111) *A* surface, the XPS results show that there are about two Se emitters for every Ga emitter that is not paired with an As emitter; on the (111) *B* surface the ratio of Se to excess Ga is about 1.7. If the Se simply replaced As or was deposited as stoichiometric GaSe, the Se:excess-Ga ratio

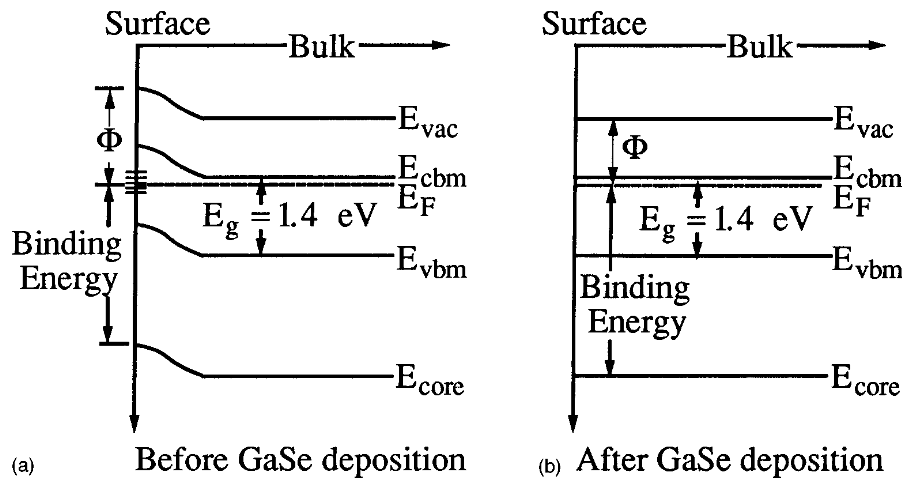

FIG. 12. Relationship between the electronic band structure of and the measured XPS spectrum. (a) Surface dangling bonds act as electrical defects that pin the Fermi level near the midband gap. (b) Termination of surface dangling bonds result in a return toward a flat-band condition.

would be 1. A Se monolayer covering the entire surface in addition to 0.5 ML of GaSe would have a Se:Ga ratio of 2:1; if it only covered the substrate beneath the GaSe, the ratio would be 1.5:1 (times a factor accounting for inelastic scattering). The observed intensity ratios are therefore consistent with termination of the GaAs surface by about 1 ML of Se before the growth of GaSe. However, the total Se uptake is much larger on the GaAs (111) *A* surface than on the (111) *B* surface, as is the decrease in the As 3*d* emission. This is strong evidence for a Se–As replacement reaction below the surface bilayer on the (111) *A* surface.

We propose that Se interdiffusion may be enhanced by the local Ga vacancy structure on the (111) *A* surface. A replacement reaction between Se and As followed by As reevaporation would also explain the very rapid reduction in the As emission intensity compared to growth on the (111) *B* surface. On the GaAs (100) surface, exposure to H_2Se (Ref. 47) or Ga+Se_x (Refs. 48 and 49) and the growth of ZnSe (Refs. 50 and 51) have been shown to produce Ga_2Se_3 in the near-surface region. Ga_2Se_3 is based on the zinc-blende lattice of GaAs, with Se sitting on the anion sites and every third Ga site vacant. This is a similar structure to the vacancy reconstruction already present on the GaAs (111) *A* surface, which may enhance its nucleation. However, Ga_2Se_3 would lead to a Se:excess-Ga ratio of 1.5, indicating that additional Se beyond that required for the sesquiselenide is present, for example, one or more monolayers of Se at the surface.

These results are consistent with previous photoemission experiments exposing GaAs(100) (Refs. 40, and 42–44) and (111) (Ref. 40) surfaces to pure Se. Using surface-sensitive, high-resolution photoemission, two Se species separated by about 1.0 eV are observed for Se on GaAs(100), (111) *A*, and (111) *B*. Both the total Se intensity and the relative size of the lower binding energy Se component are largest for the (111) *A* surface, followed by those of the (100) and (111) *B*.[40] These results were attributed to a full monolayer of Se for each surface, with the amount of additional buried Se (in a replacement reaction) depending on the surface. The persistence of this behavior in the presence of a stoichiometric Ga:Se ratio incident on the surface demonstrates the dominance of the chemical driving forces for the reaction of Se with the GaAs substrate. This is similar to the As termination of Si(111) during GaAs growth on that substrate.[52]

One molecular layer (ML) of GaSe consists of two Ga and two Se atomic layers (Se–Ga–Ga–Se), so that 0.5 ML deposition of GaSe (as Ga_2Se+Se_2) could result in a complete monolayer of Ga_1Se_1 on the substrate. It is not possible to distinguish between this possibility and a replacement reaction between Se_2 and surface [(111) *B*] or subsurface [(111) *A*] As while Ga_2Se does not stick. However, the observed appearance of RHEED streaks at the GaSe lattice constant at 0.5 ML deposition for both GaAs(111) *A* and (111) *B* and the disappearance of the high-binding energy components at the completion of a Ga_2Se_2 molecular layer on GaAs(111) *B* indicate that Ga_2Se_2 layers are forming at an early stage.

C. Growth model

Our model of the growth initiation process on the two GaAs(111) surfaces is shown schematically in Fig. 11. The incident Ga_2Se and Se_2 flux impinge on the heated GaAs surface. At the (111) *B* surface, both Se_2 and Ga_2Se react with the surface, although more Se sticks than Ga. The Se fills As vacancies and completes the surface bilayer, recruiting Ga as needed from the Ga_2Se_2 species that initially react with surface asperities. The surface likely becomes smoother by these reactions. Our data are consistent with the $Se_{0.75}As_{0.25}$ stoichiometry in the surface layer needed to remove states that pin the Fermi level; the removal of these states is confirmed by the shift in the bulk GaAs energy toward flat-band conditions. Once the reactive dangling bonds are removed, stoichiometric, crystalline GaSe layers nucleate and grow. Some Se interdiffusion may occur, but it is not as extensive as that for the (111) *A* surface.

Deposition of GaSe on the (111) *A* surface is shown schematically in Fig. 11 (right side). The reaction to deposit Se

occurs readily, with no observed intermediate state. This could be due either to the absence of reaction sites for Ga_2Se or to the location of the Se adsorption site above the native reconstruction (instead of as a replacement reaction). Se still replaces As, however, in the subsurface layers. While the XPS intensities obtained by the CMA cannot be compared directly when more than one depth is involved, roughly twice as much Se appears to be present at the GaSe/GaAs(111) A interface than at the GaSe/GaAs(111) B interface. This replacement would account for the apparent increase in deposition rate observed based on attenuation of the As signal, since loss of As from the substrate would result in a misleading rate value.

Further exposure to the GaSe flux results in the formation of stoichiometric GaSe for both the (111) A and (111) B substrates. Both GaAs(111) and GaSe(0001) have hexagonal surface symmetry with a 6% lattice mismatch, thus deposition of GaSe on GaAs(111) results in a 6% increase in the RHEED streak spacing. Upon further deposition (>one layer), the GaSe pattern becomes more evident as GaSe molecular layers are deposited. This is shown schematically in Fig. 11(c).

V. CONCLUSION

Using a combination of RHEED and XPS, the deposition of GaSe on GaAs(111) A and (111) B surfaces was studied. From this work, it is concluded that termination of the GaAs dangling bonds by Se occurs prior to the formation of GaSe. No evidence for Se–As bonding was observed with XPS, but what was seen was a Se–As replacement reaction. Subsequent deposition results in the formation of rotationally aligned, stoichiometric GaSe layers, overcoming a lattice mismatch of 6% for GaAs(111) A and GaAs(111) B.

Se reaction with the substrate results in a passivated surface on which the GaSe layered material can nucleate. This passivation process occurs *in situ* during the deposition process and chemically driven prior to the formation of GaSe. This passivation process appears to be the same as that observed when GaAs is exposed to only Se (Ref. 40) or when As termination precedes GaAs deposition on Si(111).[52] In this study, exposure to a GaSe flux results in Se termination of the GaAs substrate dangling bonds. In addition, RHEED observations of this process indicate that only GaAs and GaSe structures are present, with the GaSe forming its own lattice spacing within the first layer of growth.

The growth behavior on the (111) A and B surfaces were similar in that single orientation GaSe was formed on each surface. However, an increased uptake of Se into the GaAs(111) A substrate was found. On the GaAs(111) B substrate, Se termination at the initial stage of deposition results in an immediate return toward a flat-band condition as surface dangling bonds are passivated. This observation suggests a $GaSe_{0.75}As_{0.25}$ stoichiometry for the surface bilayer. At submonolayer coverages, high-binding energy components were observed for As, Se, and Ga and were attributed to Ga_2Se bonding to surface As.

On the (111) A substrate, the increased interdiffusion of Se into the bulk makes the termination process more difficult to observe. The substrate band bending is in the same direction as that observed for the (111) B substrate. However, the shift is gradual and occurs during the deposition of four layers of GaSe. This slow band bending has been associated with Se interdiffusion, with the Se acting as an n-type dopant in the GaAs. Results of XPS intensities indicate that on the order of one monolayer of Se is trapped at the interface in addition to this interdiffusion.

ACKNOWLEDGMENTS

This work was partly supported by NSF Grant Nos. ECS-9209652 and ECS-9414298 and by the Japanese New Energy and Industrial Technology Development Organization (NEDO).

[1] A. Koma, K. Sunouchi, and T. Miyajima, J. Vac. Sci. Technol. A **3**, 724 (1985).
[2] A. Koma, K. Ueno, and K. Saiki, J. Cryst. Growth **111**, 1029 (1991).
[3] F. S. Ohuchi, T. Shimada, B. A. Parkinson, K. Ueno, and A. Koma, J. Cryst. Growth **111**, 1033 (1991).
[4] F. S. Ohuchi, B. A. Parkinson, K. Ueno, and A. Koma, J. Appl. Phys. **68**, 2168 (1990).
[5] R. Schlaf, S. Tiefenbacher, O. Lang, C. Pettenkofer, and W. Jaegermann, Surf. Sci. **303**, L343 (1994).
[6] R. Schlaf, D. Louder, O. Lang, C. Pettenkofer, W. Jaegermann, K. W. Nebesny, P. A. Lee, B. A. Parkinson, and N. R. Armstrong, J. Vac. Sci. Technol. A **13**, 1761 (1995).
[7] O. Lang, A. Klein, R. Schlaf, T. Loher, C. Pettenkofer, W. Jaegermann, and A. Chevy, J. Cryst. Growth **146**, 439 (1995).
[8] O. Lang, R. Schlaf, Y. Tomm, C. Pettenkofer, and W. Jaegermann, J. Appl. Phys. **75**, 7805 (1994); O. Lang, Y. Tomm, R. Schlaf, C. Pettenkofer, and W. Jaegermann, *ibid.* **75**, 7814 (1994).
[9] A. Kuhn, A. Chevy, and R. Chevalier, Phys. Status Solidi A **31**, 469 (1975).
[10] F. Levy, *Structural Chemistry of Layer-type Phases*, Vol. 5 Physics and Chemistry of Materials with Layered Structures (Reidel, Dordrecht, Holland, 1976).
[11] R. Le Toullec, N. Picciolo, M. Mejatty, and M. Balkanski, Nuovo Cimento B **38**, 159 (1977).
[12] G. A. Akhundov, A. A. Agaeva, V. M. Salmanov, Y. P. Sharonov, and I. D. Yaroshetskii, Sov. Phys. Semicond. **7**, 826 (1973).
[13] I. M. Catalan, A. Cingolini, A. Minafra, and C. Paorici, Opt. Commun. **24**, 105 (1978).
[14] N. C. Fernelius, Prog. Cryst. Growth Charact. Mater. **28**, 275 (1994).
[15] K. Ueno, T. Shimada, K. Saiki, and A. Koma, Appl. Phys. Lett. **56**, 327 (1990).
[16] A. Miyata, M. Shimura, and T. Okumura, Mem. Fac. Tech. Tokyo Metropol. Univ. **41**, 4465 (1991).
[17] K. Ueno, H. Abe, K. Saiki, and A. Koma, Jpn. J. Appl. Phys., Part 2 **30**, L1352 (1991).
[18] K. Ueno, H. Abe, K. Saiki, A. Koma, H. Oigawa, and Y. Nannichi, Surf. Sci. **267**, 43 (1992).
[19] N. Kojima, K. Sato, A. Yamada, M. Konakai, and K. Takahashi, Jpn. J. Appl. Phys., Part 2 **33**, L1482 (1994).
[20] L. E. Rumaner and F. S. Ohuchi, in *Compound Semiconductor Epitaxy*, edited by C. W. Tu, L. A. Kolodziejski, and V. R. McCrary (Materials Research Society, Pittsburgh, 1994), p. 537.
[21] J. L. Gray, L. E. Rumaner, H. M. Yoo, and F. S. Ohuchi, in Ref. 21, p. 381.
[22] L. E. Rumaner, J. L. Gray, F. S. Ohuchi, K. Ueno, and A. Koma, in *Structure and Properties of Multilayered Thin Films*, edited by T. D. Nguyen, B. M. Lairson, B. M. Clemens, S. C. Shin, and K. Sato (Materials Research Society, Pittsburgh, 1995), p. 101.
[23] J. E. Palmer, T. Saitoh, T. Yodo, and M. Tamura, Jpn. J. Appl. Phys., Part 2 **32**, L1126 (1993); J. Appl. Phys. **74**, 7211 (1993).

[24]J. E. Palmer, T. Saitoh, T. Yodo, and M. Tamura, J. Cryst. Growth **147**, 283 (1995); **150**, 685 (1995).
[25]Y.-L. Kuang, K. Ueno, Y. Fujikawa, K. Saiki, and A. Koma, Jpn. J. Appl. Phys., Part 2 **32**, L434 (1993).
[26]K. Ueno, M. Sakurai, and A. Koma, J. Cryst. Growth **150**, 1180 (1995).
[27]L. T. Vinh, M. Eddrief, C. Sebenne, A. Sacuto, and M. Balkanski, J. Cryst. Growth **135**, 1 (1994).
[28]H. Reqqass, J. P. Lacharme, C. Sebenne, M. Eddrief, and V. Le-Thanh, Surf. Sci. **331-333**, 464 (1995); Appl. Surf. Sci. **92**, 357 (1996).
[29]A. Koebel, Y. Zheng, J. F. Petroff, M. Eddrief, L. T. Vinh, and C. Sebenne, J. Cryst. Growth **154**, 269 (1995).
[30]Y. Zheng, A. Koebel, J. F. Petroff, J. C. Bouliard, B. Capelle, and M. Eddrief, J. Cryst. Growth **162**, 135 (1996).
[31]A. Ludviksson, L. E. Rumaner, J. W. Rogers, Jr., and F. S. Ohuchi, J. Cryst. Growth **151**, 114 (1995).
[32]S. Y. Tong, G. Xu, and W. N. Mei, Phys. Rev. Lett. **52**, 1693 (1984).
[33]D. J. Chadi, Phys. Rev. Lett. **52**, 1911 (1984).
[34]K. W. Haberern and M. D. Pashley, Phys. Rev. B **41**, 3226 (1990).
[35]D. K. Biegelsen, R. D. Bringans, J. E. Northrup, and L.-E. Swartz, Phys. Rev. Lett. **65**, 452 (1990).
[36]D. A. Woolf, D. I. Westwood, and R. H. Williams, Appl. Phys. Lett. **62**, 1370 (1993).
[37]T. Fukuda and Y. Hirota, J. Vac. Sci. Technol. B **11**, 1982 (1993).
[38]Loss of As is also accompanied by desorption of Ga or formation of pools of Ga on the surface. This results in exposure of the next As layer, and does not result in a Ga terminated surface. It is not possible to remove the surface layer of As and change the surface from a (111) *B* to a (111) *A* surface.
[39]M. G. Lagally, D. E. Savage, and M. C. Tringides, in *Proceedings of a NATO Advanced Research Workshop on Reflection High Energy Electron Diffraction and Reflection Electron Imaging of Surfaces*, edited by P. K. Larsen and P. J. Dobson (Plenum, New York, 1987), p. 139.
[40]T. Scimeca, Y. Watanabe, R. Berrigan, and M. Oshima, Phys. Rev. B **46**, 10 201 (1992).
[41]T. Ohno, Phys. Rev. B **44**, 6306 (1991).
[42]S. A. Chambers and V. S. Sundaram, Appl. Phys. Lett. **57**, 2342 (1990); J. Vac. Sci. Technol. B **9**, 2256 (1991).
[43]S. Takatani, T. Kikawa, and M. Nakazawa, Phys. Rev. B **45**, 8498 (1992).
[44]F. Maeda, Y. Watanabe, T. Scimeca, and M. Oshima, Phys. Rev. B **48**, 4956 (1993).
[45]The Ga 3*d* intensity for GaSe is larger than that for GaAs (see Fig. 6). In GaSe, there are two Ga layers per 8 Å molecular layer; in GaAs the equivalent distance is 6.5 Å. This indicates that the inelastic escape depth must be longer in GaSe than in GaAs.
[46]J. Szuber, Appl. Surf. Sci. **55**, 143 (1992).
[47]D. R. T. Zahn, A. Krost, M. Kolodziejczyk, and W. Richter, J. Vac. Sci. Technol. B **11**, 2077 (1992).
[48]T. Okamoto, A. Yamada, M. Konagai, and K. Takahashi, J. Cryst. Growth **138**, 204 (1994).
[49]D. Li, Y. Nakamura, N. Otsuka, J. Qiu, M. Kobayashi, and R. L. Gunshor, J. Cryst. Growth **111**, 1038 (1991).
[50]A. Krost, W. Richter, and D. R. T. Zahn, Appl. Phys. Lett. **57**, 1981 (1990).
[51]J. Qui, D. R. Menke, M. Kobayashi, R. L. Gunshor, Q. D. Qian, D. Li, and N. Otsuka, J. Cryst. Growth **111**, 747 (1991).
[52]R. D. Bringans, M. A. Olmstead, R. I. G. Uhrberg, and R. Z. Bachrach, Phys. Rev. B **36**, 9569 (1987).